Microstructure investigation of low carbon steel after hot deformation

N. Wolańska*, A.K. Lis, J. Lis

Institute of materials Engineering, Faculty of Materials Processing Technology
and Applied Physics, Czestochowa University of Technology,
Armi Krajowej 19, 42-200 Czestochowa, Poland
* Corresponding author: E-mail address: npiwek@mim.pcz.czest.pl

Properties

ABSTRACT

Purpose: Investigations of microstructure after hot deformation was presented in this work. The non-metallic inclusion influence on the microstructure and type of crack mechanism was shown. The hot ductility investigations were carried out on the low carbon-manganese steel with addition of boron.

Design/methodology/approach: The ductility of the steel was measured by reduction of area during the extension test in the temperature range from 700°C to 1200°C. The test was carried out with two different strain rates $0.01s^{-1}$ and $6.5s^{-1}$. The first one is characteristic for the continuous casting process and the second one for rolling of heavy plates and billets. The deformation microstructures of investigated steel after the hot extension tests were characterized by optical microscopy and scanning electron microscopy. The chemical composition of non-metallic inclusion was established by EDX analyses.

Findings: The received ~30 % ductility minimum of investigated steel with $0.01s^{-1}$ strain rate, was found in the temperature range from 900°C to 1000°C and these temperatures are connected with band straightening in the continuous casting process. The minimum of hot ductility for fast strain rate $6.5s^{-1}$ reached ~65% reduction of area value. The ferrite-bainite and ferrite-pearlite microstructures after air cooling were observed. The inclusions in diferent size from 0.6 to 4 µm and different shape (spherical and elongated) were observed. There were MnS and SiO_2 inclusions with some other elements like Al_2O_3 and MnO.

Practical implications: Low carbon steel with addition of boron is produced by continuous casting process where straightening of the strand is taken place close to 900°C. This temperature corresponds with hot ductility minimum for investigated steel.

Originality/value: Available literature concerns investigations of low carbon steels but without boron addition, which expect to have strong influence on the position of the hot ductility minimum.

Keywords: Ductility; Hot ductility curves; Non-metallic inclusions.

1. Introduction

Nowadays in practical conventional continuous casting of steel is to straighten the strand at the high temperature end of ductility trough (>900°C). All precautions are taken to edge cracking occurs. Dynamic recrystallisation cannot occur during straightening owning to the low strain (2-4%) because the improvement in ductility is much smaller then indicated by the normal tensile hot ductility curve where strains are much greater, what was presented in the work [1-5]. The minimum in the %RA-T curves (the bottom of the trough) can be used to characterize the depth and the width of the ductility trough, what gives the possibility to compare the hot ductility of different continuous cast steels slabs, and may be used to predict the steel susceptibility to transverse cracking during continuous casting in practice. Thus, a deeper and wider trough is a signal of a larger probability of transverse cracking during the unbending operation in the continuous casting machine.

Work [2] indicates that the higher bending loads may not be a problem because ferrite and austenite are present together and ferrite is softer the on austenite. The temperature needs to be about 30°C below the Ar_3 to make sure that ferrite is present before bending [1-5].

2. Experimental

The chemical composition of the continuously cast low carbon steel with boron addition is given in Table 1. The cylindrical tensile samples of 10 mm dia. and 120 mm length, were machined with their longitudinal axes parallel to the casting direction, from regions near the slab surface.

The tensil tests were performed using a Gleeble 3500 machine. The thermomechanical cycle used to simulate the straightening operation is shown schematically in Figure 1. The effect of deformation was investigated at two different strain rates. The first one is used during a continuous casting process 0.01 s^{-1} and the second one for rolling of heavy plates and billets 6.5 s^{-1}.

The cool samples were sectioned longitudinally with respect to the rolling direction for metallography of the fracture subsurface region. The deformation microstructures were characterized by optical microscopy and scanning electron microscopy with EDX technique.

3. Results

3.1. Hot ductility curves

The effect of deformation was investigated at two different strain rates. The experimental data were plotted as the reduction of area at fracture in function of the temperature (Fig. 2).As can be seen, the %RA for the investigated steel tested at temperatures below 750°C is close to 90% for both strain rates. As the temperature increases there is a rapid decrease in ductility to %RA values as low as 30% for slow deformation and 65% for fast deformation. Tensile testing at temperature greater than about 1000°C and 900°C for samples deformed with 0.01 s^{-1} and 6.5 s^{-1} strain rate respectively, caused recovery of the ductility. The loss of ductility at temperatures between 900 and 1000°C causes the %RA-T plots to exhibit a ductility trough.

3.2. Microstructure

The deformation microstructures were characterized by optical microscopy and were taken from the neck of the sample close to the failure. Structures after deformation are shown in Figures 3-5. The structure in the Figure 3 consists of ferrite and pearlite grains on the deformed prior austenite grains boundaries. In the space between the ferrite-pearlite structure the bainite grains can be seen. In the Figure 4 the structure consists of Widmanstätten ferrite on the prior austenite grain boundaries and bainite with acicular ferrite. The zig-zag shape cracks with inclusions inside can be observed. Similar structure can be observed in the Figure 5 but without cracks.
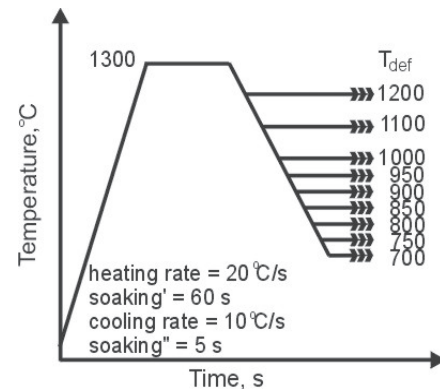
Fig. 1. Conditions of hot tensile test
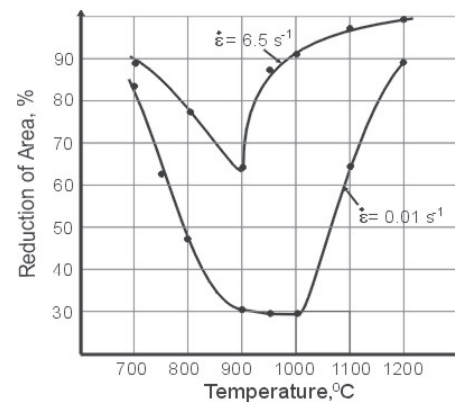
Fig. 2. The hot ductility curves

3.3. Non-metallic inclusions

The chemical composition of non-metallic inclusions was established by EDX analyses of the samples surface. The structure was taken from different parts of samples. The inclusions which were analyzed are in different sizes from 0.6 to 4 μm and mostly there are: MnS with round shape and SiO_2 in different shapes but always with some other elements like Al_2O_3 and MnO. In the Figure 6. MnS inclusion with other elements like Al and Si can be seen (1). Inclusion with 4μm in diameter occurs with a not very big void – 8μm in length – but in the neighborhood under the surface there is a bigger microcrack on the grain boundary. There is silicate oxide with diameter 0.65μm inside a ferrite grain (2) and no void around that inclusion. MnS inclusion with some silicate oxide around with diameter 1.3μm occurs on the grain boundary inside a 4μm long void (3).

Table 1.
The chemical composition of the investigated steel

C	Mn	Si	P	S	Cr
0.1	0.47	0.08	0.014	0.023	0.08
Ni	Cu	Mo	Sn	B	N
0.05	0.17	0.014	0.009	0.006	0.009
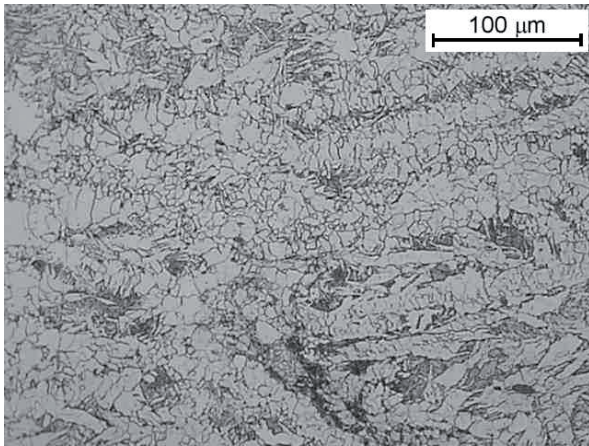
Fig. 3. Microstructure of a sample deformed at 750°C with strain rate 0.01s^{-1}
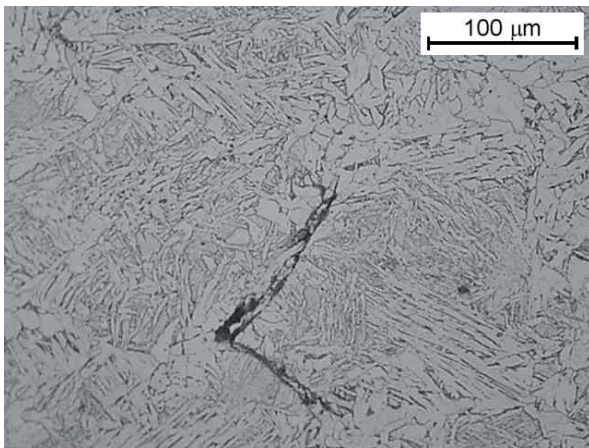
Fig. 4. Microstructure of a sample deformed at 950°C with strain rate 0.01s^{-1}
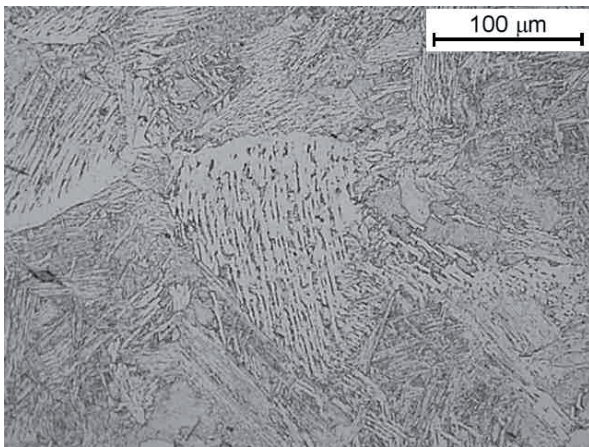
Fig. 5. Microstructure of a sample deformed at 1200°C with strain rate 0.01s^{-1}
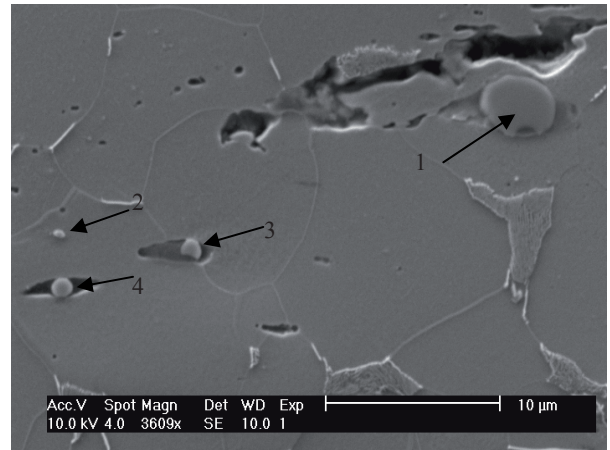
Fig. 6. Inclusions in the sample neck (sample deformed at 900°C with strain rate 6.5s^{-1})
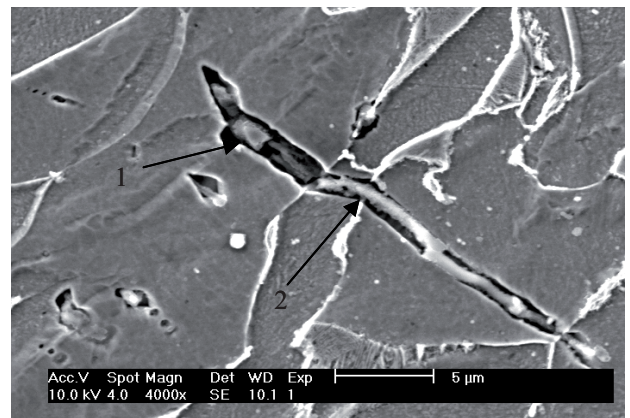
Fig. 7. Inclusions in the sample neck (sample deformed at 1200°C with strain rate 6.5s^{-1}

There was also indicated silicate oxide inside 4µm long void with a diameter of 1.3µm within a ferrite grain. In Figure 7 the whole inclusion is a complex of many elements like Al, Si, Ca, Mn, S which can create oxides and other phases. They formed a very long inclusion ~24µm length. The void around it is not much longer because the inclusions fill it out almost completely and it is situated through three grains.

Inclusions occur in the structure in different places e.g. inside the grains but also at the grain boundary. In the sample neck they are always inside voids, where the influence of deformation occurred.

4. Discussion

The microstructure in the sample neck depends on the test temperature and the strain rate of deformation. In the lower temperature of deformation (700-900^{0}C) there were austenite and ferrite in the structure. Above those temperatures there was only austenite in the sample structure before deformation. The volume

fraction of ferrite grains increase with the decrease of the temperature and the ductility grows as well. In the hot ductility minimum austenite and nuclei of ferrite grains are present in the structure during deformation at 900ºC. In the zone of hot ductility minimum the microstructure is changed to the Widmanstätten ferrite on the prior austenite grain boundaries and bainite with acicular ferrite [6-8]. In this zone the zig-zag shaped cracks with inclusions inside can be found. In the zone above minimum of hot ductility the microstructure is made of very long needle-shaped ferrite grains. The cracks which were observed in the minimum of the hot ductility do not appear at those test temperatures. That is because of dynamic recrystalization of austenite.

The inclusion have been known to be detrimental to the mechanical properties of steel since they act as nucleation sites for microvoids and cracks [9-12]. However the role of some fine inclusions as inoculants has attracted much attention and certain inclusions dispersed in steel can provide potential sites for the heterogeneous nucleation of intergranular ferrite during the austenite-ferrite transformation what could provide to possibility of controlling the microstructure and mechanical properties of steel. There have been some non-metallic inclusions reported to be potent for the nucleation of intergranular ferrite such as Ti_2O_3, SiO_2, Al_2O_3, $MnO \cdot SiO_2$, MnS, TiN, VN but the potency of some inclusions isn't clear [13,14]. Shin et al. found that allotriomorphic ferrite was formed along prior austenite grain boundaries and that the austenite-ferrite transformation did not propagate significantly from prior austenite grain boundaries into austenite grains. And a large number of intergranular polygonal ferrite islands are also observed which were indicated by non-metallic inclusions.

The most frequent inclusions in the present steel are sulphides. Sulphide creates with iron the precipitation of FeS, which may cause cracking during plastic deformation and because of that manganese is added to the chemical composition of steel. MnS occurs in steel in different forms: from round shape to irregular angular shape and often has varying amount of other elements in solid solution [15,17]. In the investigated steel, MnS occurs alone but sometimes with other elements surrounding it or inversely (Fig. 6, 7). The shape and percentage deformation depends not only on the applied force but also of the elements with which MnS creates the duplex inclusions [15]. MnS could change its shape by heat-treatment [15-17]. In our case soaking time equals only 60 seconds at 1300˚C and we can affirm that during the heating process inclusions were not fully dissolved.

Other inclusion in the investigated steel were observed in systems, which can be classified as $MnO-SiO_2-Al_2O_3$ and $CaO-SiO_2-Al_2O_3$ systems well discussed in [15]. These inclusions were formed during melting and are thermodynamically stable during reheating experiments up to 1300˚C. The silicate containing inclusions have much higher plasticity than those without silicate. Silicate creates elongated forms (Fig. 7) and harder parts are only broken up or stay undeformed.

5. Conclusions

The hot ductility minimum of low carbon steel containing boron for strain rates 0.01 s^{-1} and 6.5 s^{-1} were found in the temperature range 900ºC to 1000ºC and 900ºC respectively. The ductility trough of low C-Mn-B steel in the temperature range 700–1200 ºC becomes deeper and wider as strain rate of deformation is lowered. This hot ductility drop of investigated steel can caus difficulties in hot working during continuous casting processing.

The inclusions like MnS, SiO_2, Al_2O_3, MnO in different size from 0.6 to 4 μm and round and elongated shape were found.

References

[1] A. Cowley, R. Abushosha, B. Mintz, Influence of Ar3 and Ae3 temperatures on hot ductility of steel, Materials Science and Technology, 14 November (1998) 1145-1153.

[2] B. Mintz, Importance of Ar3 temperature in cintroling ductility and width of hot ductility trough in steels and its relationship to transverse cracking, Materials Science and Technology 12 February (1996) 132-138.

[3] B. Mintz, A. Cowley, R. Abushosha, Importance of columnar grains in dictating hot ductility of steels, Materials Science and Technology 16 (2000) 1-5.

[4] B. Mintz, The influence of composition on the hot ductility of steels and to the problem of transverse cracking, ISIJ International 39 (1999) 833-855.

[5] C.M. Chimani, K. Morwald, Micromechanical investigation of the hot ductility behavior of steel, ISIJ International 39 (1999) 1194-1197.

[6] M. Carsi, M.T. Larrea, F. Panalba, Characterization of medium carbon microalloyed steels with boron, AMTT, Zakopane, (1995) 95-100.

[7] R. Nowosielski, P. Sakiewicz, P. Gramatyka, The effect of ductility minimum temperature in CuNi25 alloy, AMME 2005, Gliwice-Wisła, Poland, 487-492.

[8] H.K.D.H. Bhadeshia, Bainite in steels, The University Press, Cambridge, London, 2001.

[9] R. Nowosielski, P. akiewicz, J. Mazurkiewicz, Ductility Minimum Temperature phenomenon in as cast CuNi25 alloy, Journal of Achievements in Materials and Manufacturing Engineering 17 (2006) 193-196.

[10] W. Ozgowicz, The relationship between hot ductility and intergranular fracture in an CuSn6P alloy at elevated temperatures, AMME 2005, Gliwice-Wisła, Poland,503-508.

[11] S.M. Pytel, Hot ductility of continuous cast structural steels, AMTT, Zakopane, 1995, 403-411.

[12] J.Sojka, P. Betakova, L. Hyspecka, L. Cizek, M. Sozańska, A. Hernas, Role of non-metallic inclusion shape in hydrogen embitterment tested Rusing slow strain rate test, AMME 2003, Gliwice-Zakopane, Poland, 821-824.

[13] J. Shim, Y. Oh, J. Suh, Y. Cho, J. Shim, J. Byun, D. Lee, Ferrite nucleation potency of non-metallic inclusions in medium carbon steels, Acta Materialia 49 (2001) 2115-2122.

[14] J.H. Shim, Y.W. Cho, S.H. Chung, J.D. Shim, D.N. Lee, Nucleation of intragranular ferrite at Ti2O3 particle in low carbon steel, Acta Materialia 47 (1999) 2751-2760.

[15] R. Kiessling, N. Lange, Non metallic inclusion in steel. Second edition, The Institute of Materials, London, 1997.

[16] B. Garbarz, J. Marcisz, J. Wojtas, TEM analysis of fine sulphides dissolution and precipitation in steel, Materials Chemistry and Physics 81 (2003) 486-489.

[17] L.A. Dobrzański, The engineering materials and materials design, WNT, Warszawa, 2006.